CIVIL ENGINEERING JOURNAL

Article no. 35

THE CIVIL ENGINEERING JOURNAL 4-2024

RESEARCH ON THE COMBINED DAMPING TECHNOLOGY OF SHALLOW BURIED LARGE-SECTION LOESS TUNNEL

Xuansheng Cheng[1], Kai Ding[1], Haodong Sun[2] and Peiyan Xia[2]

1. *Key Laboratory of Disaster Prevention and Mitigation in Civil Engineering of Gansu Province, Lanzhou University of Technology, Lanzhou, 730050, PR China, 231081402007@lut.edu.cn*
2. *Western Engineering Research Center of Disaster Mitigation in Civil Engineering of Ministry of Education, Lanzhou University of Technology, No. 287, Langongping Road, Lanzhou 730050, China*

ABSTRACT

Due to the unique characteristics of loess and the higher seismic performance requirements for tunnel engineering, researching the seismic response of loess tunnels with vibration reduction measures is essential. This study is based on the Xicheng Mountain Tunnel project, employing finite element software to establish a three-dimensional numerical model. It analyzes the stress and strain responses of the structure under different spacing of shock absorption joints and varying stiffness of the lining. A combination of " rigid lining + shock absorption joint " is proposed, and the effectiveness of this combined vibration reduction strategy is further analyzed. The results indicate that installing shock absorption joints can significantly reduce the dynamic response of loess tunnels during seismic activity, with a recommended joint spacing of 10 meters, which can reduce maximum structural stress by up to 46%. Different lining stiffness leads to varied dynamic responses; as stiffness increases, structural stress rises, while deformation decreases. A rigid lining can increase structural stress by 28.7%, but can also reduce strain by 47.5%. The combined approach of " rigid lining + shock absorption joint " effectively harnesses the advantages of individual vibration reduction measures, reducing both stress and strain, thereby mitigating seismic risks to loess tunnels.

KEY WORDS

Shallow buried, Large cross-sectio,; Loess tunnel, Lining stiffness, Shock absorption joint

INTRODUCTION

Since 2003, urban rail transit construction in China has experienced rapid development [1], with numerous tunnel projects implemented in loess regions. Several tunnels, such as the Maqu Tunnel of the Yinkun Expressway and the Xichengshan Tunnel of the Tianzhuang Expressway, have been completed in these areas. Loess tunnels are structures built under loess geological conditions. The complex particle composition, large pore spaces, and loose structure of loess pose significant challenges for tunnel construction, maintenance, and seismic mitigation. Therefore, studying the seismic response of tunnel structures under anti-vibration measures is crucial for the seismic design and reinforcement of tunnel engineering in loess regions.

Early research suggested that underground structures possess good seismic resistance due to the constraints provided by surrounding soil, often leading to the application of above-ground

seismic design methods for preliminary assessments. However, the widespread damage to underground structures during the 1995 Hyogo-ken Nanbu (Kobe) earthquake [2] heightened awareness of the impact of earthquakes on these structures. This event prompted global seismologists to focus on seismic damage to underground structures, leading to in-depth investigations into the damage mechanisms of tunnels and subway stations, as well as the development of relevant analytical theories and design methods. Consequently, a surge in research on underground tunnel seismic resistance has emerged. Current studies [3-6] predominantly utilize numerical simulation methods to analyze the stress deformation and failure mechanisms of tunnel structures under seismic loads, including various types such as mountain tunnels, underwater tunnels, and shield tunnels. Hassani et al. [7-8] conducted nonlinear seismic analyses using the pseudo-static method and damage concrete models in ABAQUS. Sun et al. [9] proposed a method for determining the height of the pressure arch above tunnels based on changes in surrounding rock stress during seismic events. Basirat et al. [10-11] employed various analytical and numerical methods to study the interaction between tunnel linings and surrounding media under seismic loads. As seismic analysis methods for underground structures have evolved, the application of model testing has become increasingly widespread. Studies by Cui et al. [12-16] indicate that implementing damping layers and expansion joints can significantly reduce displacements and stresses in tunnel linings. Additionally, novel anti-seismic measures proposed by Li et al. [17-18], based on large-scale quasi-static and shaking table tests, have examined the dynamic response characteristics of tunnel structures. While these studies provide a solid foundation for understanding the seismic response and stability of tunnel structures, most focus on rock tunnels, and the applicability of existing findings to loess tunnels, given their unique physical properties, remains to be further explored.

Research on seismic mitigation measures for loess tunnels has included contributions from Zhou et al. [19], who conducted a 1/40 scale model test to investigate the effects of damping layers on loess tunnel structures. Sun et al. [20] performed a 1:25 scale model test focused on off-axis loess tunnels, analyzing the seismic response and failure modes of their slopes and off-axis sections. Sun et al. [21] centered their research on the amplification effects of seismic waves in the soil surrounding tunnel portals under strong seismic conditions, employing numerical simulations to explore the acceleration and displacement responses of lining structures and proposing recommended lengths for seismic protection. Cheng et al. [22-23] examined the seismic response characteristics of loess tunnels under the influence of EI-Centro seismic waves and rainfall infiltration, determining locations for seismic reinforcement measures based on peak stress, displacement, and pore water pressure. Overall, existing research primarily focuses on enhancing linings and incorporating damping layers, while studies on shock absorption joints remain limited. Given that shock absorption joints are commonly used in tunnel seismic design, further investigation into their application in loess tunnels is essential. Therefore, it is necessary to conduct in-depth research on shock absorption joints within loess tunnels to develop more reliable, economical, and implementable seismic measures, thereby providing scientific basis and technical support for the seismic protection of loess tunnel structures.

This study employs numerical simulation methods to examine the seismic response of loess tunnels under individual damping measures. Furthermore, it proposes a combined damping measure of "shock absorption joints + rigid lining" and analyzes the effectiveness of this approach in mitigating seismic effects on loess tunnels. The research findings aim to enhance the rationality and economy of seismic design for loess tunnels.

NUMERICAL MODEL

Analysis model

This paper relies on the Xichengshan tunnel project of the Zhuanglang-Tianshui section of the highway, which is located in Qingshui County, Tianshui City (see Figure1). The tunnel is located in the collapsible loess area with a large thickness. According to the field engineering geological survey data, the total length of the tunnel is 4080 m, the buried depth of the tunnel in the loess area is 20 m ~ 30 m, and the diameter of the hole is 9 m. According to the International Tunnel Association (ITA) and the " Specifications for Design of Highway Tunnels " definition of tunnel cross-sectional area and buried depth (see Table 1 and Table 2), the tunnel is divided into shallow-buried large-section tunnels. The model analysis diagram is shown in Figure 2, where h1 is the distance from the tunnel to the top of the model at 20 m, h2 is the distance from the tunnel to the bottom of the model at 51 m, a is the distance from the tunnel to the boundary of the model at 45.5 m, and D is the tunnel diameter of 9 m. To minimize the boundary effects on the seismic response of underground structures, the calculation width of the site should be larger than the structure width by 5 times [24]. Considering the boundaries of the tunnel, the overall dimensions of the model are 100m × 80m × 60m (length × width × height). To achieve more accurate numerical simulation results, the element grid size should be smaller than 1/10 to 1/8 of the wavelength [25]. The finite element analysis model is shown in Figure 3.

Fig.1- Tunnel scene pictures

Tab. 1 - Tunnel depth division standards

	Shallow-buried tunnel	Deep-buried tunnel	Ultra-deep tunnel
Depth range（m）	<（2~3）h_q	>（2~3）h_q~500m	> 500m

where h_q is the critical depth, which determines whether the top cover layer of the tunnel can form a pressure arch [26].

Tab. 2 - Tunnel cross-section division standards

	Minimal cross-section tunnel	Small cross-section tunnel	Medium-section tunnel	Large cross-section tunnel	Extra-large cross-section tunnel
Cross-sectional area（m^2）	2~3m^2	3~10m^2	10~50m^2	50~100m^2	> 100m^2

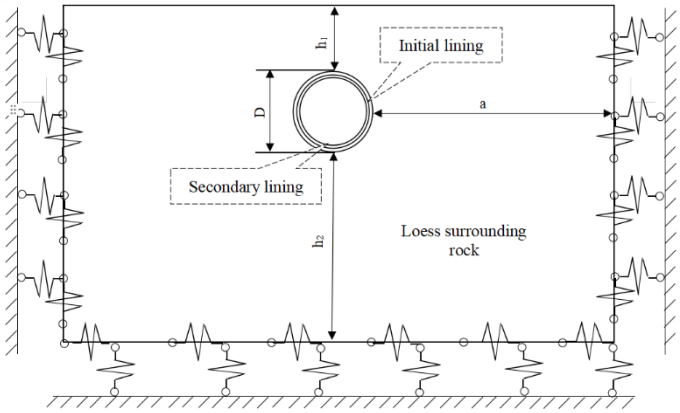

Fig.2 - Model analysis diagram

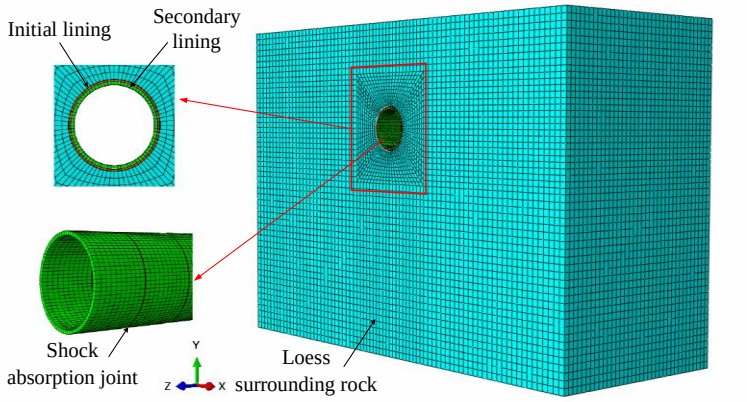

Fig. 3 - Finite element analysis model

To study the seismic response of underground structures, this research approximates the foundation as a semi-infinite space and selects a finite computational domain for dynamic analysis. To address boundary fluctuations and scattering issues at low frequencies, and to eliminate the seismic wave effects caused by truncated boundaries, viscoelastic artificial boundaries are applied around the model and at its base. Based on these boundary conditions, the seismic loads are converted into equivalent nodal forces, which are then applied to the sides and bottom of the model. The specific calculation formula for viscoelastic boundary conditions is as follows [27]:

$$\left.\begin{aligned} K_{BT}=\alpha_T\frac{G}{R},\quad C_{BT}=\rho C_s \\ K_{BN}=\alpha_N\frac{G}{R},\quad C_{BN}=\rho C_p \end{aligned}\right\} \qquad (1)$$

where K_{BT}, K_{BN} are the stiffness coefficients of tangential springs and normal springs; C_{BT}, C_{BT} are the damping coefficients of tangential dampers and normal dampers; α_T, α_N are the correction coefficients of viscoelastic boundaries; R is the distance from the wave source to the artificial boundary point; ρ, G are the density and shear modulus of the medium respectively; C_s, C_p are the shear wave velocity and longitudinal wave velocity of the medium.

Material parameters

This study employs ABAQUS finite element software for modeling the tunnel structure. The surrounding rock is simulated using solid elements with the Mohr-Coulomb constitutive model,

effectively capturing the material behavior under shear and normal stress conditions. The mechanical parameters of the surrounding rock are detailed in Table 3 [22]. The lining is also modeled using solid structural units, adopting an elastic constitutive model to reflect its response to seismic loads. The initial support comprises 28 cm thick C30 shotcrete, while the secondary lining consists of 50 cm thick C50 reinforced concrete. A shock absorption joint, 20 cm wide, is incorporated into the secondary lining, segmenting it and filling the segments with soft rubber plates. An elastic constitutive model is used to represent the deformation characteristics of the rubber plates accurately. The relevant mechanical parameters are presented in Table 4 [26]. The interaction between the surrounding rock and the initial lining is established using the Coulomb contact model, which effectively captures the frictional behavior at the interface. The normal contact behavior is defined as hard contact to prevent penetration, with a tangential contact friction coefficient set at 0.446. The Coulomb contact model is also applied between the initial and secondary linings to ensure realistic interactions under dynamic loading conditions, with a tangential friction coefficient of 0.3 [16].

Tab. 3 - Rock mass mechanics parameters

	Density ρ/kg/m^3	Elastic modulus E/MPa	Poisson ratio υ	Cohesion c/kPa	Internal friction angle φ/°
Loess	1800	60	0.35	61.2	28.9

Table 4 Material mechanics parameters

Supporting type	Type	Volumetric weight γ/kg/m^3	Elastic modulus E/MPa	Poisson ratio υ	Thickness /cm
Conventional lining	Initial lining	23.5	18000	0.25	28
	Secondary lining	25	28000	0.20	50
Rigid lining	Initial lining	25	43000	0.25	28
	Secondary lining	27	54000	0.20	50
Flexible lining	Initial lining	21	8000	0.25	28
	Secondary lining	23	17000	0.20	50
	shock absorption joint	10	8	0.45	20

Damping measures

In the anti-seismic design of a tunnel, the strength of the surrounding rock is the key to determining the choice of anti-seismic measures. When the surrounding rock condition is poor, grouting reinforcement can be used to improve the strength of the surrounding rock. At the same time, the thickness of the lining can be increased or the stiffness of the lining can be changed within a certain range to reduce the seismic response of tunnel structure. When the tunnel is subjected to a strong earthquake, the above measures cannot meet the requirements of tunnel seismic resistance, it is necessary to improve the seismic resistance of the tunnel by setting the damping layer or the shock absorption joint in the structure.

The tunnel is located in Tianshui City, Gansu Province, in a loess area with poor surrounding rock conditions. According to the "Seismic ground motion parameters zonation map of China" (GB18306) [28], the basic peak ground acceleration for this region is 0.3g. Therefore, this study adopts a peak ground acceleration of 0.3g, considering it as a strong earthquake effect. To address this, damping measures such as the installation of expansion joints and adjustments to lining stiffness have been implemented. The existing research results have proved that the damping effect

of the initial lining setting shock absorption joint on the tunnel is not obvious [12]. In this paper, the shock absorption joint is only set on the secondary lining, and the damping effect of the single damping measure on the loess tunnel is analyzed by changing the spacing of the shock absorption joint and the stiffness of the lining. At the same time, the combined damping method of " rigid lining + shock absorption joint " is proposed, and the damping effect is analyzed, which provides a reference for the anti-seismic design of the loess tunnel.

Ground motion

The El-Centro wave is selected as the seismic wave, and the baseline correction of the seismic acceleration time history is carried out by Seismosignal software. The 20 s including the peak acceleration of the seismic wave is intercepted, and the time interval is 0.02 s. The adjusted seismic wave acceleration time history curve is shown in Figure 4. For the viscoelastic artificial boundary, the existing research shows that the difference between the numerical calculation results and the analytical solution is large by using the acceleration input method or the displacement input method, and both of them will cause the boundary condition to fail. However, the equivalent nodal force input method is used, and the calculation results are consistent with the theoretical solution, and the calculation accuracy is high [29]. Using viscoelastic boundary conditions, the seismic load needs to be converted into equivalent nodal force applied to the boundary nodes. The dynamic equilibrium equation is :

$$Mu_t'' + Cu_t' + Ku_t = F_b \quad (2)$$

where M, C, and K are the mass matrix, damping matrix, and stiffness matrix of the system respectively; u_t is the displacement of the incident wave at the boundary; F_b is the applied equivalent nodal force, which can be calculated by the following equation:

$$F_b = \left(K_b u_b^f + C_b u_b'^f + \varphi_b^f n\right) A_b \quad (3)$$

Where u_b^f and $u_b'^f$ are the free field displacement and velocity vector caused by the input seismic wave on the viscoelastic boundary node respectively; φ_b^f is the free field stress tensor; n is the outer normal direction residual vector of viscoelastic boundary; A_b is the control area of the nodes on the viscoelastic boundary [30].

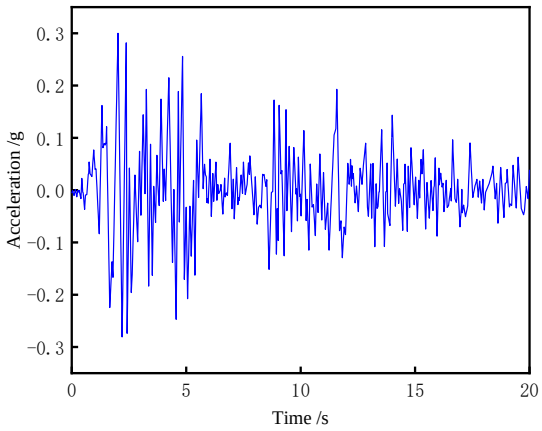

Fig. 4 - Acceleration time history curve

In this paper, based on the calculation formula of equivalent nodal force, the ground motion input program of infinite element boundary is compiled, and the input of ground motion is realized by applying equivalent nodal force at the bottom of the model.

RESULTS ANALYSIS AND DISCUSSION

Calculation conditions

Eight calculation models of condition I ~ condition IX are established. The distance from the tunnel boundary to 5 m, 10 m, 15 m, 20 m, 25 m, 30 m, 35 m, 40 m, 45 m, 50 m, 55 m and 60 m is selected as the monitoring section. The data of the vault, arch shoulder, arch waist, and inverted arch of each monitoring section under different working conditions are extracted, and the maximum principal stress peak and maximum principal strain peak of the lining structure are analyzed. To facilitate the comparison, the eight working conditions are divided into three groups for comparison. Working conditions I, II, III, and IV are the first group, working conditions I, V, and VI are the second group, and working conditions I, VII, and IX are the third group.

Tab. 5 - Calculation conditions

Condition number	Condition details	Condition number	Condition details
I	No damping measures	V	Flexible lining
II	Shock absorption joint spacing is 10 m	VI	Rigid lining
III	Shock absorption joint spacing is 15m	VII	Flexible lining + Shock absorption joint
IV	Shock absorption joint spacing is 20m	IX	Rigid lining + Shock absorption joint

Although the damping measures have an impact on the relative displacement value of the tunnel structure, the degree of influence is small and can be ignored in practical engineering applications. Therefore, the displacement analysis plays an auxiliary role, and the damping effect should be analyzed mainly by referring to the variation law of stress and strain.

Stress

The maximum principal stress peak of each part of the lining structure during the earthquake action time is extracted, and the data of different damping measures are drawn according to the grouping, as shown in Fig.5, Fig.6, and Fig.7. The upper left corner of the figure displays the cross-section of the tunnel, where the black dots represent the locations of the monitoring points, corresponding to the vault, arch shoulder, arch waist, and inverted arch.

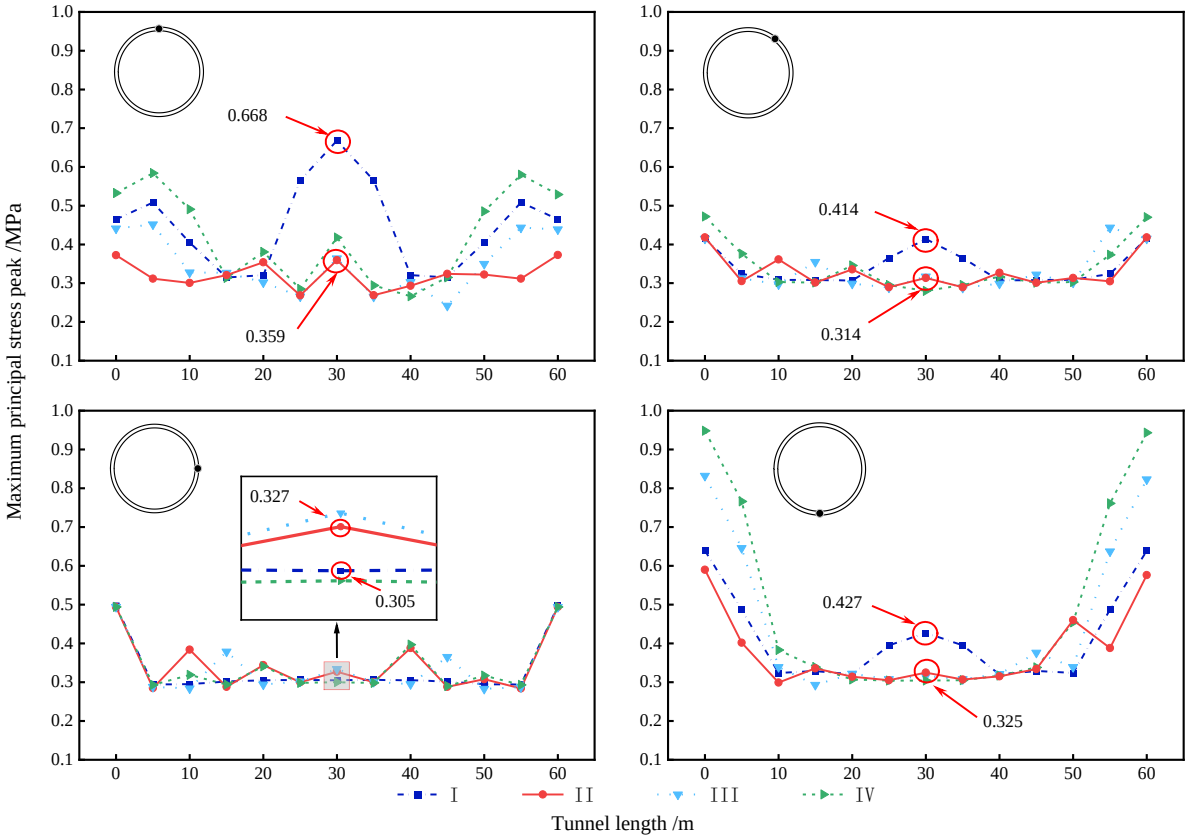

Fig. 5 - The peak principal stress of the lining structure is distributed along the longitudinal direction after the shock absorption joint is set

It can be seen from Figure 5 that the shock absorption joint can significantly change the seismic response of each part of the lining structure. Along the longitudinal length of the tunnel, the change amplitude of the vault and the inverted arch is larger, while the change law of the arch shoulder and the arch waist is similar. Considering that the tunnel can be simplified to analyze the simply supported beam, the deformation in the middle of the tunnel is large. The monitoring section data at the length of 30 m are extracted for analysis. After the shock absorption joint is set, the maximum principal stress peak of each part of the lining structure is significantly reduced. Compared with the three working conditions of 10 m, 15 m, and 20 m respectively, the smaller the spacing of the shock absorption joint is, the more obvious the damping effect is. When the spacing of the shock absorption joint is 10 m, the vault is reduced by 0.31 MPa, and the reduction rate is 46 %. The arch shoulder is reduced by 0.1 MPa, and the reduction rate is 24 %. The arch waist is reduced by 0.02 MPa, and the reduction rate is 6.7 %. The inverted arch is reduced by 0.1 MPa, and the reduction rate is 23.9 %.

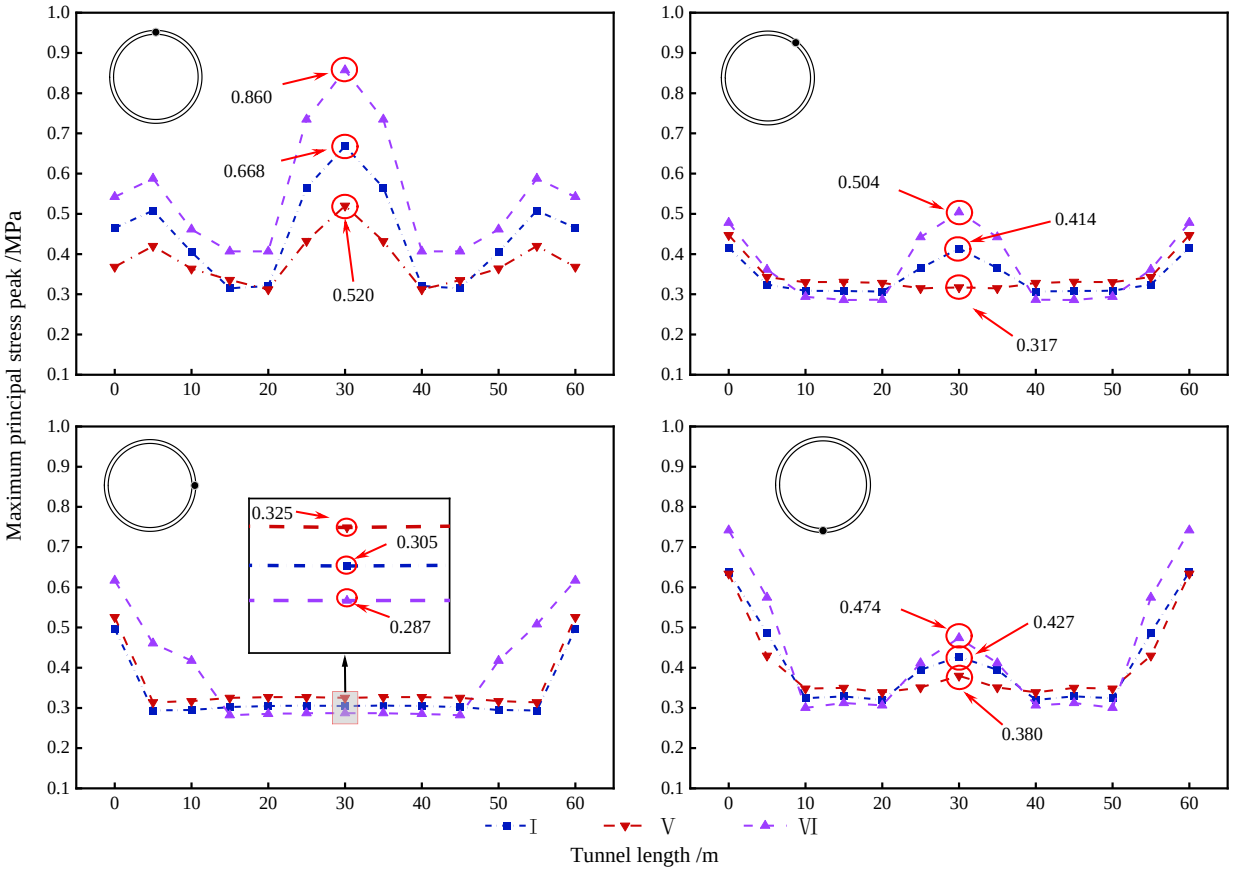

Fig. 6 - The peak principal stress of lining structure with different stiffness are distributed along the longitudinal direction

It can be seen from Figure 6 that the seismic response of the lining structure with different stiffness is different. Along the longitudinal length of the tunnel, the variation rules of the three working conditions are the same, that is, the vault and arch shoulder reach the maximum in the middle of the tunnel, while the arch waist and inverted arch reach the maximum at both ends of the tunnel. The tunnel is also regarded as a simply supported beam to extract the monitoring section data at 30 m for analysis. Compared with the conventional lining, the flexible lining significantly reduces structural stress. The vault is reduced by 0.15 MPa, the reduction rate is 22.2 %, the arch shoulder is reduced by 0.1 MPa, the reduction rate is 23.4 %, the inverted arch is reduced by 0.05 MPa, the reduction rate is 11.3 %, and the stress at the arch waist is increased by 0.02 MPa, and the increase is small. The rigid lining increases the structural stress, in which the vault increases by 0.19 MPa, the increase rate is 28.7 %, the arch shoulder increases by 0.1 MPa, the increase rate is 21.7 %, the inverted arch increases by 0.05 MPa, the increase rate is 11 %, and the stress at the arch waist decreases by 0.02 MPa, and the decrease amplitude is small. It can be concluded that the change in lining stiffness can make the peak stress of the structure change. The changing amplitude of the vault and arch shoulder is larger, while the changing amplitude of the arch waist and inverted arch is smaller. Considering that the left and right ends of the tunnel section are squeezed, the upper and lower ends are stretched.

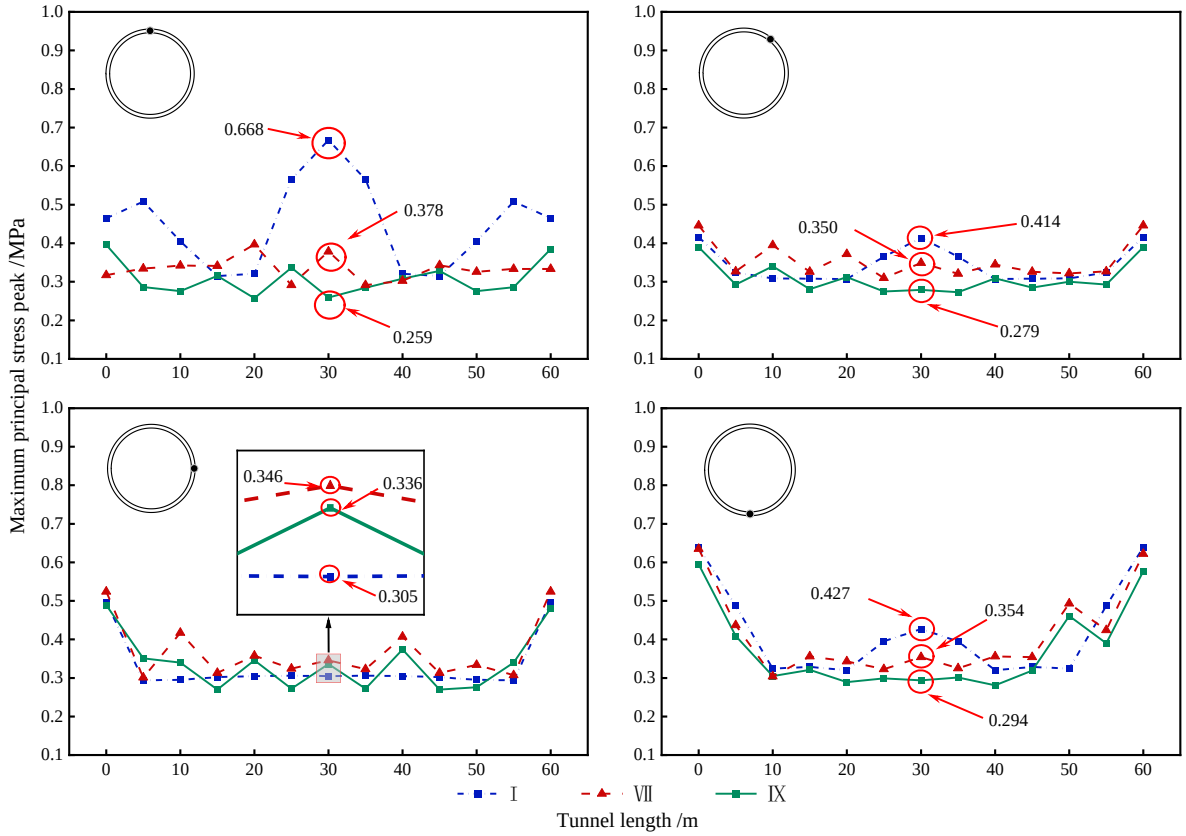

Fig. 7 - The peak principal stress of the lining structure with combined damping measures is distributed along the longitudinal direction

It can be seen from Figure 7 that the two combined damping measures can reduce the stress of the tunnel to a certain extent. Along the longitudinal length of the tunnel, the variation rules of the two damping measures are the same, and the change range is the largest at the 30 m position of the tunnel. The monitoring section data at this position are analyzed. The combined damping measures of flexible lining + shock absorption joint can reduce the stress of the vault of the structure by 0.29 MPa, the reduction rate is 43.4 %, the arch shoulder is reduced by 0.06 MPa, the reduction rate is 15.5 %, and the inverted arch is reduced by 0.07 MPa, the reduction rate is 17.1 %, while the change amplitude at the arch waist is small. The combined damping measures of rigid lining + shock absorption joint can reduce the stress of the vault of the structure by 0.41 MPa, with a reduction rate of 61.2 %, the arch shoulder by 0.14 MPa, with a reduction rate of 32.6 %, and the inverted arch by 0.13 MPa, with a reduction rate of 31.1 %.

Strain

The maximum principal strain peak of each part of the lining structure during the earthquake action time is extracted, and the data of different damping measures are drawn according to the grouping, as shown in Figure 8, Figure 9, and Figure 10.

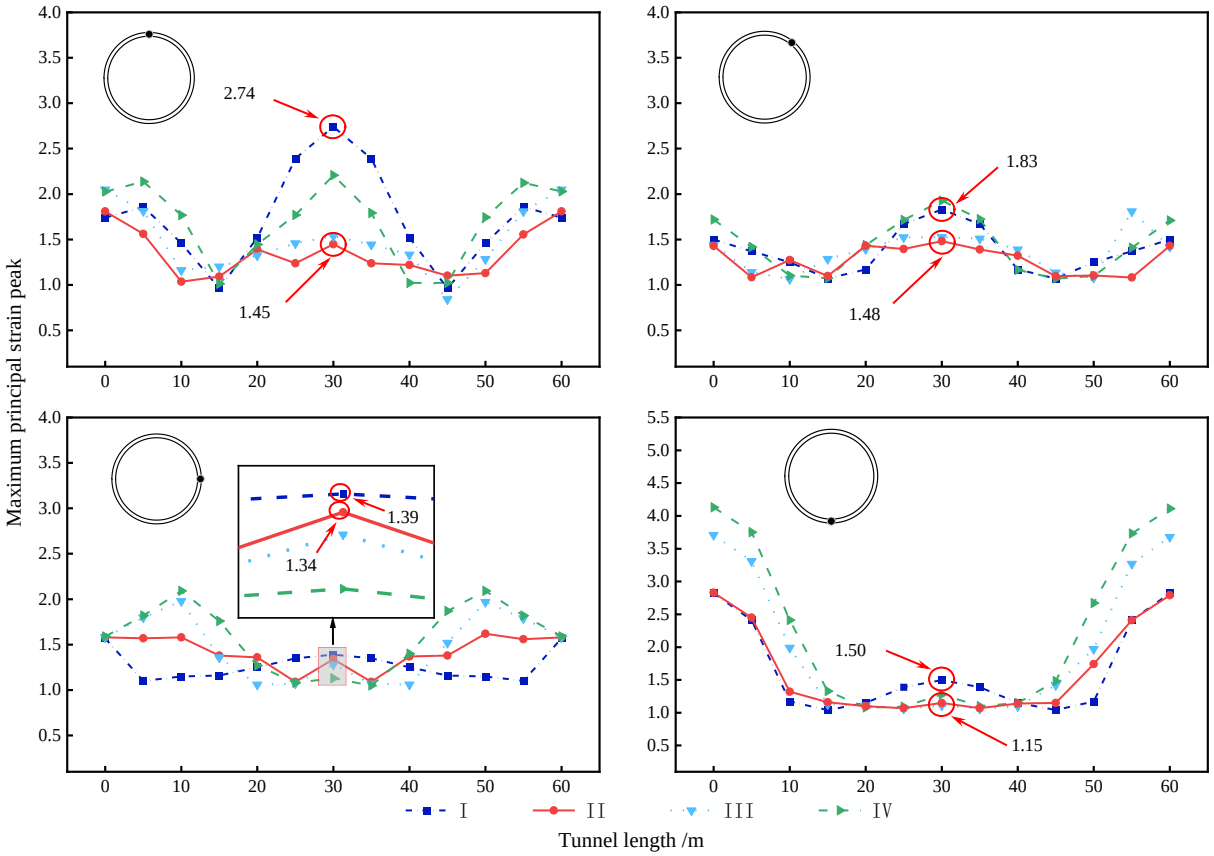

Fig. 8 - The main strain peaks of the lining structure are distributed along the longitudinal direction after the shock absorption joint is set.

It can be seen from Figure 8 that with the change of stress, the strain of the lining structure after setting the shock absorption joint also changes greatly. The change law is similar to the change law of stress. The vault and arch shoulder change greatly in the middle of the tunnel, and the arch waist and inverted arch change greatly at both ends of the tunnel. Along the longitudinal length of the tunnel, the change range of the strain peak curve of each part of the structure after setting the shock absorption joint is significantly reduced, and the tunnel deformation along the longitudinal direction is more uniform. The monitoring section data at 30 m is extracted for analysis. When the spacing of the shock absorption joint is 10 m, the vault is reduced by 47 %, the arch shoulder is reduced by 19 %, and the inverted arch is reduced by 23 %, while the change amplitude at the arch waist is small.

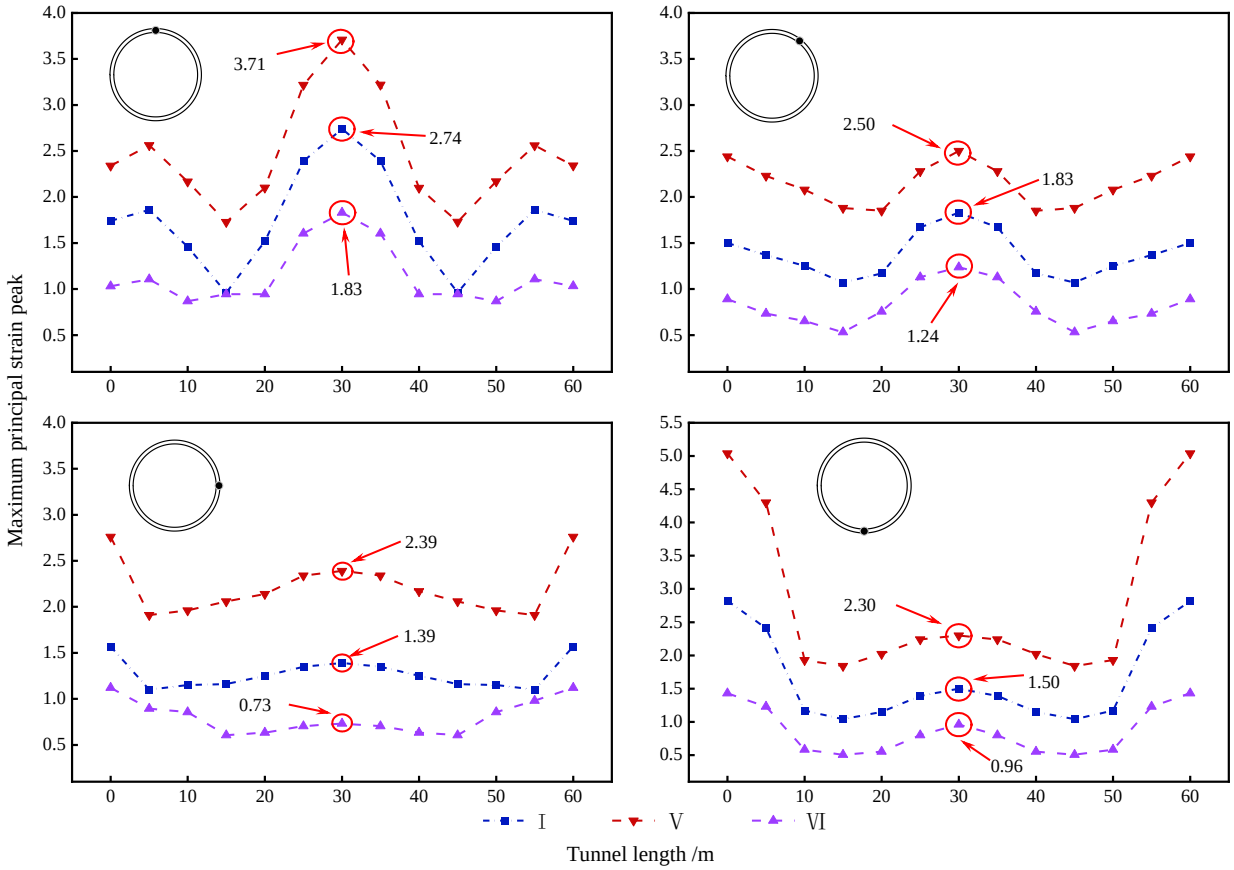

Fig. 9 - The main strain peaks of lining structures with different stiffness are distributed along the longitudinal direction.

It can be seen from Figure 9 that the lining stiffness is different, and the deformation law of the structure along the longitudinal distribution is similar, but the strain peaks are different. The monitoring section data at 30 m were extracted for analysis. Compared with the conventional lining, although the flexible lining reduced the structural stress, the structural deformation increased significantly. The maximum principal strain at the vault increased by 35.4 %, the arch shoulder increased by 36.6 %, the arch waist increased by 71.9 %, and the inverted arch increased by 54.4 %. On the contrary, the rigid lining significantly reduces the structural deformation, in which the maximum principal strain at the vault is reduced by 33 %, the arch shoulder is reduced by 32 %, the arch waist is reduced by 47.5 %, and the inverted arch is reduced by 36 %. It can be concluded that the strength of the rigid lining material is large, although the force is large, the deformation is small, and it has a good supporting effect on the surrounding rock.

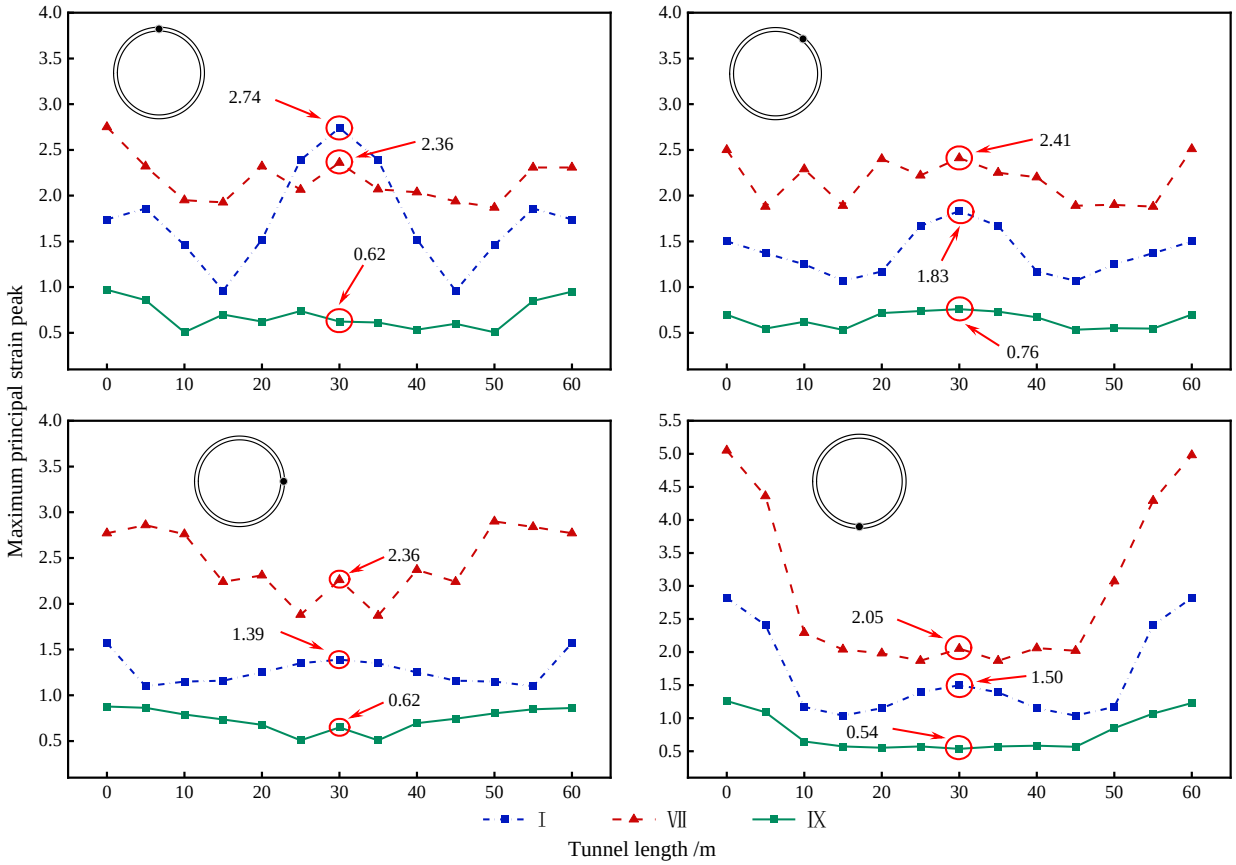

Fig. 10 - The main strain peaks of the lining structure with combined damping measures are distributed along the longitudinal direction.

According to the analysis of Figure 10, except for the vault, the combined damping measures of flexible lining + shock absorption joint increase the peak strain of each part of the structure, while the strain of the vault at both ends of the tunnel increases and the strain at the middle section decreases. The combined damping measures of rigid lining + shock absorption joint reduce the peak strain of each part of the structure. The data of the monitoring section at 30 m were extracted for analysis. The flexible lining + shock absorption joint measure increased the strain at the arch shoulder of the structure by 31.7 %, the arch waist by 69.7 %, and the inverted arch by 36.7 %, while the reduction amplitude at the vault was small. The rigid lining + shock absorption joint measures reduce the strain at the vault of the structure by 73.7 %, the arch shoulder by 58.5 %, the arch waist by 55.4 %, and the inverted arch by 64 %. It can be concluded that the combined damping measures of rigid lining + shock absorption joint can effectively reduce the structural deformation, and the reduction amplitude is large. Compared with the conclusion of the shaking table model test carried out by Xin[13], the higher the strength of the lining concrete, the better the damping effect of the damping joint, which is consistent with the conclusion of the study.

Table 6 summarizes the effects of various damping measures. In the table, “+” indicates an increase, while “-” indicates a decrease.

Tab.6 - Summary of damping measures effects

Damping measures	Type	Location	Stress	Strain
Shock absorption joint	Spacing is 10 m	Vault	-46%	-47%
		Arch shoulder	-24%	-19%
		Inverted arch	-23.9%	-23%
Lining stiffness	Flexible lining	Vault	-22.2%	+35.4%
		Arch shoulder	-23.4%	+36.6%
		Inverted arch	-11.3%	+54.4%
	Rigid lining	Vault	+28.7%	-33%
		Arch shoulder	+21.7%	-32%
		Inverted arch	+11%	-36%
Combined damping measures	Flexible lining + Shock absorption joint	Vault	-43.4%	+10.1%
		Arch shoulder	-15.5%	+31.7%
		Inverted arch	-17.1%	+36.7%
	Rigid lining + Shock absorption joint	Vault	-61.2%	-73.7%
		Arch shoulder	-32.6%	-58.5%
		Inverted arch	-31.1%	-64%

According to the analysis in Table 6, the installation of shock absorption joints significantly affects the seismic response of tunnel lining structures. Along the tunnel's longitudinal direction, the stress variation is more pronounced at the crown and the arch, while the shoulder and waist exhibit similar trends. When comparing different joint spacing (10m, 15m, and 20m), a smaller spacing results in a more noticeable damping effect; at a joint spacing of 10m, the stresses at the crown, shoulder, and arch decrease by 46%, 24%, and 23.9%, respectively. The stiffness of the lining structure has a significant impact on dynamic response, with flexible linings reducing the stresses at the crown and shoulder by 22.2% and 23.4%, respectively, while slightly increasing the stress at the waist. Conversely, rigid linings generally lead to an increase in structural stress. Both combinations of damping measures (“shock absorption joint + flexible lining” and “shock absorption joint + rigid lining”) effectively reduce structural stress, with the former reducing crown stress by 43.4% and the latter achieving a reduction of 61.2%. As stress decreases, the strain behavior also shows consistent trends, particularly with the “shock absorption joint+ rigid lining” combination, which significantly reduces deformation. In summary, the choice of combination between shock absorption joints and lining materials is crucial for the performance of tunnel structures under seismic loads and is consistent with related research findings, indicating that the combination of high-strength concrete and seismic joints yields a more significant damping effect.

CONCLUSIONS

1) Under the action of seismic load, the maximum deformation of the lining structure of the loess tunnel mostly occurs at the vault position, that is, the stress peak and strain peak are large at this position, and the structural stress is large. This position is a weak point of the loess tunnel structure and should be strengthened during seismic design.

2) The shock absorption joint can effectively release the internal force of the structure and achieve energy dissipation. The smaller the spacing of the shock absorption joint is, the better the damping effect is. However, too small spacing will divide the tunnel into too many segments, thus destroying the integrity of the structure. This paper recommends that the spacing of shock absorption joints in loess tunnels should be 10 m.

3) The flexible lining can reduce the stress of the structure, but the strain increases, and the strain at some parts of the structure increases by more than 30 %. Although the rigid lining increases the structural stress, the strain decreases, and the strain at some positions of the structure can be reduced by more than 20 %. For the damping design of the loess tunnel, although the rigid lining increases the internal force of the structure, the bearing capacity of the loess surrounding rock is stronger, the displacement deformation of the structure is reduced, and the structure is safer.

4) Compared with flexible lining + shock absorption joint, the combined damping measures of rigid lining + shock absorption joint can give full play to the advantages of a single damping measure, so that the relative displacement of the structure in the dynamic response is reduced, and the maximum principal stress is reduced, so that the deformation of the structure is reduced, which is more suitable for the anti-seismic design of the loess tunnel.

5) This study provides an in-depth exploration of seismic mitigation techniques for loess tunnels; however, it has some limitations. First, the analysis primarily focuses on specific seismic load conditions and does not consider the effects of broader seismic scenarios and soil characteristics on structural performance. Second, the filling materials used in seismic joints significantly impact their effectiveness, but this study does not compare various damping materials. Additionally, the long-term effects and maintenance requirements of the seismic measures have not been adequately discussed. Future research should address the structural response characteristics under different types of earthquakes, explore more flexible design solutions, and consider environmental impacts and material durability to further enhance the seismic resilience of loess tunnels.

DATA AVAILABILITY

All data, models, and code generated or used during the study appear in the submitted article.

ACKNOWLEDGMENTS

This research is supported in part by the National Natural Science Foundation of China (grant number: 52178389).

REFERENCES

[1] Zhao J P, Tan Z S, Yu R S, et al. Mechanical responses of a shallow-buried super-large-section tunnel in weak surrounding rock: A case study in Guizhou[J]. TUNNELLING AND UNDERGROUND SPACE TECHNOLOGY, 2023, 131. DOI: https://doi.org/10.1016/j.tust.2022.104850.

[2] Samata S, Ohuchi H, Matsuda T. A study of the damage of subway structures during the 1995 Hanshin-Awaji earthquake[J]. CEMENT & CONCRETE COMPOSITES, 1997, 19(3):223-239. DOI: https://doi.org/10.1016/S0958-9465(97)00018-8..

[3] Wang Y, Wang Q, Zhong X M, et al. Seismic response analysis of the Daliang tunnel during the Menyuan Ms 6.9 earthquake[J]. CHINA EARTHQUAKE ENGINEERING JOURNAL, 2023, 45(6):1315-1323,1332. DOI: https://doi.org/10.20000/j.1000-0844.20230202003.

[4] Yan Y, The tunnel damage effects and implications of the coseismic rupture of Menyuan Ms 6.9 Earthquake in Qinghai, China[J]. JOURNAL OF GEOMECHANICS, 2023, 29(6):869-878. DOI: https://doi.org/10.12090/j.issn.1006-6616.2023027.

[5] Shen Y S, Gao B, Yang X M, et al. Seismic damage mechanism and dynamic deformation characteristic analysis of mountain tunnel after Wenchuan earthquake[J]. ENGINEERING GEOLOGY, 2014, 180: 85-98, DOI:https://doi.org/10.1016/j.enggeo.2014.07.017.

[6] Li Z Y. Study on vibration effect of pre-splitting crack in tunnel excavation under thermal explosion loading[J]. CASE STUDIES IN THERMAL ENGINEERING, 2021, 28: 101401. DOI:https://doi.org/10.1016/j.csite.2021.101401.

[7] Hassani R, Hojatkashani A, Basirat R. Nonlinear Seismic Analysis of Ground Structure to Evaluate the Capacity of a Permanent Tunnel Lining[J]. STRUCTURAL ENGINEERING INTERNATIONAL, 2024, 34(1): 102-113. DOI:https://doi.org/10.1080/10168664.2022.2125485.

[8] Zhou T L, Dong C S, Fu Z P, et al. Study on Seismic Response and Damping Performance of Tunnels with Double Shock Absorption Layer[J]. KSCE JOURNAL OF CIVIL ENGINEERING. 2022, 26(5): 2490-2508. DOI: https://doi.org/10.1007/s12205-022-1862-y.

[9] Sun C X, Jiang T, Lv X C, et al. Effect of Earthquake on Pressure Arch above the Tunnel[J]. LITHOSPHERE, 2021, 7: 9576745, DOI: https://doi.org/10.2113/2022/9576745.

[10] Basirat R, Salari-rad H, Molladavoodi H. Analysis of the monolithic and segmental tunnel lining under earthquake loading[J]. INGEGNERIA SISMICA, 2019, 36(4):140-155.

[11] Haque M F, Ansary M A. Liquefiable concrete tunnel-sand-pile interaction response under seismic excitations[J].GEOTECHNICAL AND GEOLOGICAL ENGINEERING, 2024, 42(1): 409-431. DOI:https://doi.org/10.1007/s10706-023-02580-9

[12] Cui G Y, Wang M N, Yu L, et al. Model test study of shock absorption joint damping technology of crossing stick-slip fracture tunnel[J]. CHINESE JOURNAL OF ROCK MECHANICS AND ENGINEERING, 2013, 32(8): 1604-1608. DOI: https://do i.org/10.3969/j.issn.1000-6915.2013.08.012.

[13] Xin C L, Gao B, Zhou J M, et al. Shaking table tests of conventional anti-seismic and damping measures on fault-crossing tunnels[J]. CHINESE JOURNAL OF ROCK MECHANICS AND ENGINEERING, 2014, 33(10): 2048-2054. DOI: https://doi.org/10.13722/ j.cnki.jrme.2014.10.011.

[14] Wen H Y, Zhou Z Y, Li X M, et al. Evaluation of the damping layer between the tunnel lining and surrounding rock via a shaking table test[J]. SUSTAINABILITY, 2023, 15: 13244. DOI: https://doi.org/10.3390/su1517132 44.

[15] Wang J, Hu Y L, Fu B Y, et al. Study on antiseismic effect of different thicknesses of shock absorption layer on urban shallow buried double arch rectangular tunnel [J]. SHOCK AND VIBRATION, 2022, 4863756, DOI: https://doi.org/10.1155/2022/4863756.

[16] Huang C X, Wang X H, Zhou H, et al. Damping effects of different shock absorbing materials for tunnel under seismic loadings[J]. JOURNAL OF VIBROENGINEERING, 2019, 21(5): 1353-1372. DOI: https://doi.org/10.21595/jve.2019.20495

[17] Li P P, Qiu W E, Lu F, et al. Quasi-static test study of tunnel with resistance-limiting shock absorption layer in high-intensity seismic[J]. FRONTIERS IN EARTH SCIENCE. 2023, 10: 1029929, DOI: https://doi.org/10.3389/feart.2022.1029929.

[18] Gui G Y, Song B H, Wang D Y. Seismic model test research on the combination of rigidity with flexibility of tunnel portal in high intensity seismic areas[J]. GEOMATICS NATURAL HAZARDS & RISK. 2021, 12(1): 1195-1211. DOI: https://doi.org/10.1080/19475705.2021.1921057.

[19] Zhou X H, Cheng X S, Qi L, et al. Shaking Table Model Test of Loess Tunnel Structure under Rainfall[J]. KSCE JOURNAL OF CIVIL ENGINEERING. 2021, 25(6): 2225-2238. DOI: https://doi.org/10.1007/s12205-021-1064-z.

[20] Sun W Y, Yan S H, Ma Q G, et al. Dynamic response characteristics and failure mode of a bias loess tunnel using a shaking table model test[J]. TRANSPORTATION GEOTECHNICS. 2021, 31: 100659, DOI: https://doi.org/10.1016/j.trgeo.2021.100659.

[21] Sun W, Liang Q G, Liu Q X, et al. Amplification effect of the portal section of loess tunnels under strong earthquake[J]. CHINA EARTHQUAKE ENGINEERING JOURNAL, 2021, 43(4): 936-941. DOI: https://doi.org/10.3969/j.issn.1000-0844.2021.04.935.

[22] Cheng X S, Zhou X H, Wang P, et al. Shaking table model test of loess tunnel[J]. CHINA J. HIGHW. TRANSP., 2021, 34(6): 134-145. DOI: https://doi.org/10.19721/j.cnki.1001-7372.2021.06.014.

[23] Cheng X S, Zhou X H, Liu H B, et al. Numerical analysis and shaking table test of seismic response of tunnel in a loess soil considering rainfall and traffic load[J]. ROCK MECHANICS AND ROCK ENGINEERING. 2021, 54(3):1005-1025. DOI: https://doi.org/10.1007/s00603-020-02291-0.

[24] Xu Z, Du X, Xu C, et al. Numerical research on seismic response characteristics of shallow buried rectangular underground structure[J]. SOIL DYNAMICS AND EARTHQUAKE ENGINEERING, 2019, 116: 242-252. DOI:https://doi.org/10.1016/j.soild yn.2018.10.030.

[25] Ma C, Lu D, Du X. Seismic performance upgrading for underground structures by introducing sliding isolation bearings[J]. TUNNELLING & UNDERGROUND SPACE TECHNOLOGY, 2018, 74: 1-9. DOI:https://doi.org/10.1016/j.tust.2018.01.007.

[26] JTG 3370.1-2018. Specifications for design of highway tunnels Section 1 Civil engineering[S]. INDUSTRY STANDARDS OF CHINA, 2019.

[27] Liu J B, Li B. Three-dimensional viscoelastic static-dynamic unified artificial boundary[J]. SCIENCE IN CHINA SER E ENGI NEERING & MATERIALS SCIENCE. 2005, 35(9): 966-980. DOI: https://doi.org/10.3321/j.issn:1006-9275.2005.09.008.

[28] GB 18306-2015. Seismic ground motion parameters zonation map of China[S]. NATIONAL STANDARDS OF CHINA, 2015.

[29] Ma S J, Chi M J, Chen H J, et al. Implementation of viscous-spring boundary in ABAQUS and comparative study on seismic motion input methods[J]. CHINESE JOURNAL OF ROCK MECHANICS AND ENGINEERING, 2020, 39(7): 1446-1455. DOI: https://doi.org/10.13722/j.cnki.jrme.2019.1068.

[30] Liu J B, Du Y X, Yan Q S. Realization of viscoelastic artificial boundary and ground motion input in general finite element software [C]. Civil Engineering Society, Proceedings of the Third National Symposium on Earthquake Prevention and Disaster Reduction Engineering, (In Chinese).